Spin-density-wave behaviour in the $(Cr_{84}Re_{16})_{100-y}V_y$ system

BS Jacobs, ARE Prinsloo, CJ Sheppard and AM Strydom

Department of Physics, University of Johannesburg, PO Box 524, Auckland Park, 2006

E-mail address: alettap@uj.ac.za

Abstract. In this study, the possibility of tuning the $Cr_{84}Re_{16}$ alloy system to a quantum critical point through V addition is investigated, by considering the spin-density-wave behaviour in the $(Cr_{84}Re_{16})_{100-y}V_y$ alloy system with $0 \leq y \leq 14$. The evolution of Seebeck coefficient (S) as a function of temperature (T) on increasing the V content is described in terms of a simple model. This relates the temperature behaviour of S to the energy dependence of the decrease in the scattering rate of electrons by phonons and an increase in the resistivity on decreasing temperature due to a decrease in the effective charge carriers when parts of the Fermi surface area are annihilated on cooling through the Néel temperature. The temperature – composition magnetic phase diagram obtained from the $S(T)$ and previously reported $\rho(T)$ measurements depicts a critical point, occurring at $T = 0$ K for a critical V concentration $y_c = 10.5$. Specific heat measurements were used to determine the Sommerfeld coefficient (γ) as a function of V concentration (y) for this series and a minimum is observed in the $\gamma(y)$ close y_c. This is indicative of the existence of a possible quantum critical point at this concentration.

1. Introduction

The antiferromagnetic (AFM) properties exhibited by Cr and its alloys can be attributed to a linearly polarized spin-density-wave (SDW) [1]. The Fermi surface of Cr is composed of electron and hole octahedra, the nesting of which is responsible for establishing a SDW [2]. The behaviour around critical points of Cr alloys can be probed by fine tuning the parameters that influence SDW formation. The extent of nesting and the stability of the SDW depends on the electron concentration per atom (*e/a*). This parameter can easily be tuned by alloying Cr (*e/a* = 6) with other elements. In pure Cr, the electron sheet is slightly smaller than the hole sheet, resulting in a SDW that is incommensurate (I) with the lattice [2]. Alloying Cr with Re, an electron donor having *e/a* = 7, brings the size of the electron and hole Fermi sheets more in line with each other. The SDW eventually becomes commensurate (C) with the lattice. As the Re concentration is increased, the Néel temperature (T_N) first increases up to approximately 7 at.% Re and then decreases [2]. This behaviour is presently not well understood, but corresponds to that observed in CrRu [2].

Doping Cr with V (*e/a* = 5) results in suppression of spin fluctuations [3,4], lowering of resistivity [5] and destruction of the first order transition from the paramagnetic to the antiferromagnetic phase [6]. Yeh *et al.* also [7] demonstrated that Cr can be driven to a quantum critical point (QCP) by doping with V in the $Cr_{1-x}V_x$ alloy system. Characteristics typically associated with QCP can be observed in the low temperature behaviour of electrical resistivity (ρ), magnetic susceptibility (χ), Hall coefficient (R_H) and Sommerfeld coefficient of specific heat (γ) [7,8]. Recently, Reddy *et al.* reported the existence of a CSDW QCP at $z_c = 10.4$ in the $(Cr_{86}Ru_{14})_{100-z}V_z$ alloy system [9,10]. It is therefore appropriate to extend these studies to the Cr-Re system, as it has a temperature – composition ($T - c$) magnetic phase diagram similar to that of Cr-Ru [2]. For this purpose, in the present study, thermal transport and specific heat measurements were utilized to investigate the existence of a possible QCP in the $(Cr_{84}Re_{16})_{100-y}V_y$ alloy system.

2. Experimental

Polycrystalline $(Cr_{84}Re_{16})_{100-y}V_y$ alloys with $0 \leq y \leq 14$ were prepared from Cr, Re and V of mass fractional purities of 99.99%, 99.99% and 99.8%, respectively, by repeated arc melting in purified argon atmosphere. The samples were individually sealed in quartz ampoules filled with pure argon gas at low pressure. These ampoules were annealed at 1343 K for seven days and quenched in iced water. Powder X-ray diffraction (XRD) analyses confirmed the expected body centered cubic (bcc) crystal structure [11]. Electron microprobe analyses of the samples showed the actual elemental composition and good homogeneity of the alloys [11]. Samples of desired dimensions for the various measurements were prepared from the alloy ingots using spark erosion techniques. The Seebeck coefficient (S) was measured in the temperature range 2 K $\leq T \leq$ 390 K while the specific heat (C_p) was measured in the temperature range 2 K $\leq T \leq$ 80 K using the Quantum Design Physical Properties Measurement System (PPMS) incorporating appropriate measuring options.

3. Results and discussion

The temperature dependence of electrical resistivity, ρ, for $(Cr_{84}Re_{16})_{100-y}V_y$ alloys with y = 0, 5.7, 8.5 and 10.4 at.% V have been reported previously [11]. Well defined anomalies in the vicinity of T_N were observed for alloys with y = 0, 5.7 and 8.5. In general, the size of the anomaly as well as T_N decreases with increase in V concentration, becoming almost imperceptible in the y = 10.4 alloy. The anomalies, which appeared as sudden increase in resistivity on cooling through T_N, were attributed to the condensation of electron and hole Fermi surfaces during the nesting process on SDW formation. This leads to a reduction in the charge carriers available for conduction resulting in an increase in resistivity just below T_N [2].

The Seebeck coefficient is sensitive to the changes in the electronic structure and scattering mechanisms that are consequential to the AFM phase [2]. This results in a much stronger anomaly seen in the $S(T)$ curve on SDW formation compared to those observed in $\rho(T)$ [2]. Previous research on Cr alloys indicated that $S(T)$ measurements are particularly useful in locating T_N in alloys showing weak SDW anomalies near T_N [2].

Figure 1 (a) shows the temperature dependence of Seebeck coefficient, S, for $(Cr_{84}Re_{16})_{100-y}V_y$ alloys with y = 0, 4, 5.7, 8.5 and 10.4. T_N for the various samples were taken at the temperature corresponding to the minimum observed in the $dS(T)/dT$ curves, an example of which is shown in figure 1 (b) for the y = 8.5 sample. T_N obtained in this manner compares well with that obtained from the $\rho(T)$ curves for the y = 5.7, 8.5 and 10.4 alloys [11]. For the y = 0 alloy the Néel transition could not be observed in $S(T)$, as measurements using the PPMS apparatus could only be done up to 400 K. From resistivity measurements, T_N was found to be at 423 K for this alloy. Anomalies in the form of a dome, normally associated with T_N, are observed in the $S(T)$ curves for samples with y = 4, 5.7, 8.5 and 10.4. On increasing y, the magnitude of this dome is suppressed and its position shifts to lower temperatures, corresponding to a decrease in T_N. In addition to the observed T_N-dome, low temperature valleys are seen for the y = 0, 4 and 5.7 samples. The valley is initially weak and broad for y = 0, becoming more pronounced and shifting to lower temperatures on increasing y. With further increase in V concentration this valley disappears and no such anomaly is observed for the alloys with $y > 5.7$. A small low temperature dome is also seen in the y = 0 sample which is not well understood at present, but is in correspondence to that observed in a previous study [12].

In order to understand the $S(T)$ behaviour of the $(Cr_{84}Re_{16})_{100-y}V_y$ alloy series, it must be considered that for a magnetic material the absolute thermoelectric power can be approximated as [13]:

$$S = S_{pd} + S_{mag} + S_{diff}\,, \tag{1}$$

where S_{pd} is the phonon drag term, S_{mag} is the magnon drag term and S_{diff} is due to the diffusion of the electrons. The first two terms dominate at low temperatures and the latter at elevated temperatures, to such an extent that at high temperatures, $S \approx S_{\text{diff}}$. The thermopower due to carrier diffusion is given by [2,14]:

$$S = \frac{\pi^2 k_{\mathrm{B}}^2 T}{3e}\left[\frac{\partial \ln \sigma}{\partial E}\right] \tag{2a}$$

$$S \approx \frac{\pi^2 k_{\mathrm{B}}^2 T}{3e}\left[\frac{\partial \ln \Sigma}{\partial E} + \frac{\partial \ln\langle l \rangle}{\partial E}\right], \tag{2b}$$

where σ is the electrical conductivity, Σ is the area of the Fermi surface that has not been destroyed when entering the AFM SDW state, $\langle l \rangle = \langle \tau v \rangle$ the average mean free path of charge carriers over Σ, $\langle \tau \rangle$ is the relaxation time of the electron and $\langle v \rangle$ the velocity at the Fermi surface. Σ is in many cases sensitive to the energy E, but for T just below T_{N}, where a dome is observed in $\rho(T)$, the second term in equation (2b) can dominate when the electron scattering may be largely determined by $\langle l \rangle$.

In agreement to the previously investigated Cr alloys [2], $S(T)$ for the $(\mathrm{Cr}_{84}\mathrm{Re}_{16})_{100-y}\mathrm{V}_y$ alloy system show behaviour in the form of a relatively large peak associated with the Néel temperature just below T_{N}, similar to that observed in $\rho(T)$. Trego *et al.* [14] discussed this behaviour in terms of a model in which the dominant effect is the decrease in the scattering rate of electrons by phonons when the AFM phase is entered on decreasing temperature. The Fermi surface area decreases as a result of the electron and hole surfaces that are partially annihilated and this practically results in the observed increase in ρ just below T_{N} on cooling. As indicated by equation (2b), S is determined by the energy dependence of both Σ and $\langle l \rangle$. The second term of equation (2b) dominates [14] giving a net positive contribution to S at temperatures below T_{N}.

The effects of Re and V as diluents in Cr in the present alloy series, should be considered. The low temperature minima in $S(T)$ and the way in which the minima in $S(T)$ deepen with increased V content can possibly be attributed to a phonon drag component to S. This effect was shown to be of importance when alloying Cr with elements that have an atomic mass greater than that of Cr, such as Mo and W [2,14]. In addition to a peak, associated with the Néel transition observed in $S(T)$ for the Cr-Mo and Cr-W alloys, a low-temperature valley was also noticed. This valley becomes increasingly shallower on increasing the Mo or W concentration and is finally suppressed at higher concentrations [2,14]. This behaviour is attributed to a decrease in the mean free path length $\langle l \rangle$ due to the scattering by the heavier impurity. Re has an atomic mass approximately four times that of Cr and comparable to that of W and this implies that Re as an impurity in Cr will also bring about phonon drag that might contribute to the low temperature valleys observed in the $S(T)$ curves for the $(\mathrm{Cr}_{86}\mathrm{R}_{16})_{100-y}\mathrm{V}_y$ alloys, with $y = 0$, 4 and $y = 5.7$.

The $S(T)$ curves of binary Cr-V [2,14] show a clear dome just below T_{N}, but no additional minimum is seen at low temperatures in $S(T)$ of these alloys. V has an atomic mass comparable to Cr and appears to have nearly no influence on phonon drag effect as a dopant in Cr. In the current $(\mathrm{Cr}_{84}\mathrm{Re}_{16})_{100-y}\mathrm{V}_y$ alloy series, it is expected that the effect of doping with V will increasingly dominate the $S(T)$ behaviour with increasing y. An increase in V concentration also effectively reduces the Re content of the $(\mathrm{Cr}_{84}\mathrm{Re}_{16})_{100-y}\mathrm{V}_y$ alloys. These combined effects are expected to decrease possible phonon drag contributions to $S(T)$ with increasing V content, resulting in the disappearance of the low temperature valley for samples with $y \geq 8.5$ and only a positive dome is observed just below T_{N} for these alloys.

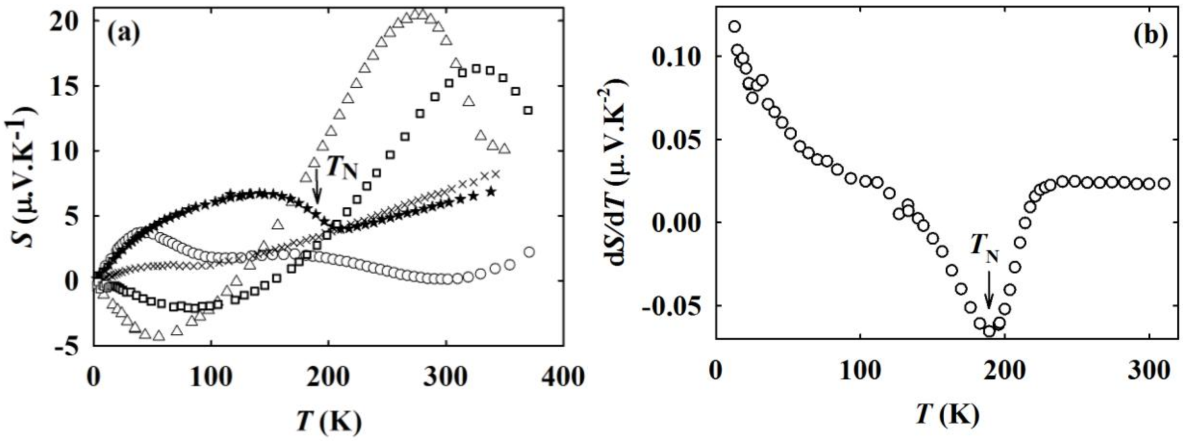

Figure 1: (a) The temperature dependence of Seebeck coefficient, S, for $(Cr_{84}Re_{16})_{100-y}V_y$ alloys with y = 0 (○), 4 (□), 5.7 (△), 8.5 (★) and 10.4 (×). (b) The temperature dependence of d$S(T)$/dT for the $(Cr_{84}Re_{16})_{91.5}V_{8.5}$ alloy. T_{N}, corresponding to the minimum in the d$S(T)$/dT curve, is marked by an arrow in figures (a) and (b) for y = 8.5.

Figure 2 shows the magnetic phase diagram for the $(Cr_{84}Re_{16})_{100-y}V_y$ alloy system. The critical concentration, y_c, for which T_N continuously tends to a zero value was obtained from a fit to the experimental data (solid line in figure), using a power law of the form $T_N = a(y_c - y)^b$, where a and b are fitting parameters. The numerical values for these fitting parameters are a = (140 ± 20) K, b = 0.49 ± 0.07 and y_c = 10.5 ± 0.0001.

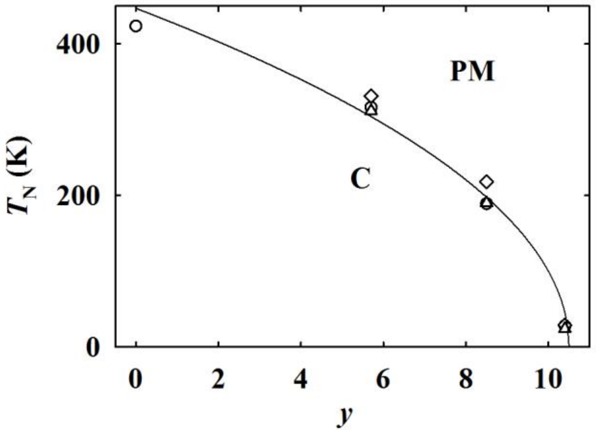

Figure 2: Magnetic phase diagram for the $(Cr_{84}Re_{16})_{100-y}V_y$ alloy system with T_N values obtained from the minima in temperature derivative of electrical resistivity (○), magnetic susceptibility (◇) and Seebeck coefficient (△) measurements. The error bars are within the size of the data points. The solid line shows a power law fit through the data.

A representative example of a specific heat (C_p) versus T curve is shown in figure 3 for the $(Cr_{84}Re_{16})_{94.3}V_{5.7}$ alloy. The Sommerfeld electronic specific heat coefficient, γ, is obtained for the $(Cr_{84}Re_{16})_{100-y}V_y$ alloy system from these measurements at low temperatures considering the equation: $C_p = \gamma T + \beta T^3$. Here, the first term represents the electronic specific heat component and the lattice contribution is represented by the second term. γ is determined from least-square fits to the low temperature specific heat measurements, giving linear behaviour for C_p/T versus T^2 in the temperature rage 2 K ≤ T ≤ 10 K, as shown by the inset of figure 3.

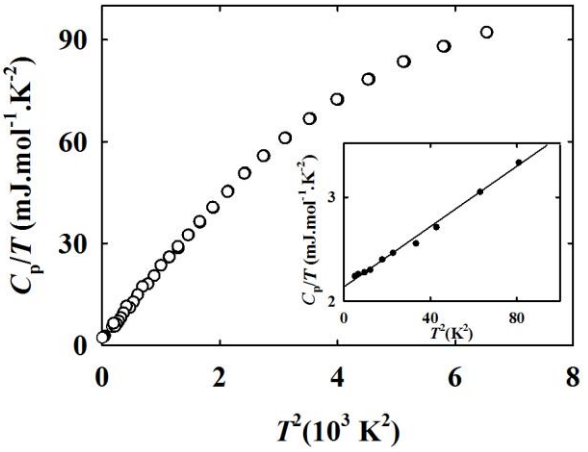

Figure 3: The dependence of C_p/T on T^2 for the $(Cr_{84}Re_{16})_{94.3}V_{5.7}$ alloy. The inset shows a linear fit through the low temperature experimental data for this alloy.

Figure 4 shows the curve of Sommerfeld electronic specific heat coefficient γ, obtained as described above, as a function of V concentration for the $(Cr_{84}Re_{16})_{100-y}V_y$ alloy system. Takeuchi *et al.* [8] reported on the behaviour of γ in the quantum critical $Cr_{1-x}V_x$ alloy system. They observed an increase in $\gamma(x)$ in the AFM phase up to the QCP where a discontinuity in $\gamma(x)$ is observed. This is followed by a gradual decrease as x is increased in the paramagnetic phase. Sheppard *et al.* [15] also observed similar behaviour below the critical concentration $z_c \approx 0.04$ in the $(Cr_{0.98}Si_{0.02})_{1-z}Mo_z$ system. In the quantum critical $(Cr_{86}Ru_{14})_{100-x}V_x$ system, Reddy *et al*. [10] observed rather unexpected behaviour in $\gamma(x)$. They reported a sharp decrease in $\gamma(x)$ in the AFM CSDW phase up to $x \approx 0.08$ followed by a jump-like increase and then a further sharp decrease of $\gamma(x)$ that continues through the critical concentration into the paramagnetic phase [10]. The behaviour of γ is thus a key indicator of quantum critical behaviour. In the $(Cr_{84}Re_{16})_{100-y}V_y$ alloy system, γ decreases on increasing y, but a minimum is observed in the $\gamma(y)$ curve at 10.4 at.% V, close to the critical concentration of $y_c = 10.5$. We are in the process of extending the research work as to include more samples as to confirm the exact concentration associated with the minimum in the $\gamma(y)$ curve.

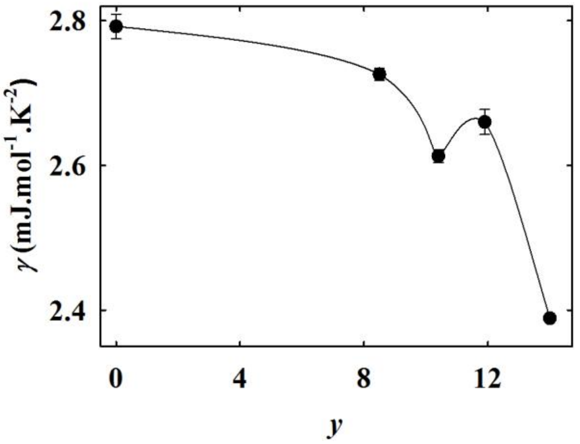

Figure 4: Sommerfeld electronic specific heat coefficient, γ, as a function of V concentration. The solid line is a guide to the eye.

4. Conclusion

Electrical resistivity and thermopower measurements on the $(Cr_{84}Re_{16})_{100-y}V_y$ alloy system indicate that V doping of $Cr_{84}Re_{16}$ reduces T_N and suppresses it down to 0 K at a critical concentration of 10.5 at.% V. Specific heat measurements were used to determine the Sommerfeld coefficient (γ) as a function of V concentration (y) for this series. A minimum is observed in the $\gamma(y)$ curve close to y_c. This is indicative of the existence of a possible quantum critical point at this concentration. However, more samples need to be prepared, especially in the region of the critical concentration. Hall coefficient and magnetic susceptibility measurements which are vital to locate and classify the QCP need to be performed to validate whether the critical point observed is a quantum critical one beyond doubt.

Acknowledgments

Financial support from the South African NRF (Grant numbers 61388 and 78832) is acknowledged.

References

[1] Galkin V Y 1991 Sov. Phys. Solid State **33** 10
[2] Fawcett E, Alberts H L, Galkin V Y, Noakes D R and Yakhmi J V 1994 *Rev. Mod. Phys.* **66** 25
[3] Dubiel S M, Cieslak J and Wagner F E 1996 *Phys. Rev.B* **55** 1
[4] Fawcett E 1992 *J.Phys.: Condens matter* **4** 923
[5] Moller H B, Trego A L and Mackintosh A R 1965 *Solid State Commun*. **3** 137
[6] Fawcett E, Roberts R B, Day R and White G K 1986 *Europhys. Lett.* **1** 473
[7] Yeh A, Soh Y A, J Brooke J, Aeppli G, Rosenbaum T F and Hayden S M 2002 *Nature* **419** 459
[8] Takeuchi J, Sasakura H and Masuda Y 1980 *J. Phys. Soc. Japan* **49** 508
[9] Reddy L, Alberts H L, Prinsloo A R E and Venter A M 2006 *J. Alloys Comp.* **426** 83
[10] Reddy L, Alberts H L, Strydom A M, Prinsloo A R E and Venter A M 2008 *J. Appl. Phys.* **103** 07C903-1
[11] Jacobs B S, Prinsloo A R E, Sheppard C J and Strydom A M 2011 *SAIP Conference Proceedings* 105
[12] Thiruvikraman P K, 1999 PhD thesis, Mangalore University
[13] Arajs S, Anderson E E and Rao K V 1971 *J. Less-Common Metals* **26** 157
[14] Trego A L and Mackintosh A R 1968 *Phys. Rev.* **166** 495
[15] Sheppard C J, Prinsloo A R E, Alberts H L and Strydom A M 2011 *J.Appl.Phys.* **109** 07E104